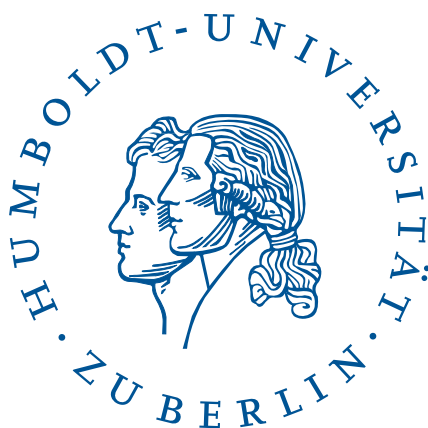


# Monodromy and Quasi-Exact Solvability of the Quantum Pendulum

## BACHELORARBEIT

zur Erlangung des akademischen Grades  
Bachelor of Science  
(B. Sc.)  
im Fach Physik



eingereicht an der  
Mathematisch-Naturwissenschaftlichen Fakultät I  
Institut für Physik  
Humboldt-Universität zu Berlin

von  
Herr Lutz Mertenskötter  
geboren am 10.1.1991 in Hamburg

Betreuung:

1. *Prof. Dr. Alejandro Saenz*
2. *Prof. Dr. Bretislav Friedrich*

eingereicht am: 18. April 2016

# Kurzfassung

Wir analysieren die Energie-Drehimpuls-Karte des quantenmechanischen Pendels um tiefere Einsicht in die Verbindung zwischen den *avoided crossings* der Eigenenergieoberflächen und der Bedingung für quasiexakte Lösbarkeit des Eigenwertproblems zu gewinnen. Es hat sich herausgestellt, dass das System sowohl im allgemeinen Fall, welcher keine analytischen Lösungen zulässt, als auch im quasiexakt lösbaren Fall nichttriviale Monodromie hat.

# Abstract

We analyze the energy-momentum map of the quantum pendulum in an attempt to deepen our understanding of the connection between the avoided crossings of its eigenenergy surfaces and the condition for the quasi-exact solvability of the quantum pendulum eigenproblem. We found that non-trivial monodromy is present not only in the general case when no analytic solutions exist but also for the quasi-exactly solvable cases.

# Contents

<b>1</b>	<b>Introduction</b>	<b>1</b>
<b>2</b>	<b>Theoretical Foundations</b>	<b>3</b>
2.1	Classically Integrable Systems and Action-Angle Coordinates . . . . .	3
2.1.1	Proof of Integrability of the Classical Quadratic Pendulum . .	3
2.1.2	The Liouville-Arnol'd Theorem . . . . .	5
2.1.3	Cusp Singular Points . . . . .	5
2.2	The Quantum Pendulum . . . . .	7
2.2.1	The Eigenvalue Problem . . . . .	7
2.2.2	The Quantum Energy-Momentum Map . . . . .	8
2.2.3	An Analysis of Numerical Errors . . . . .	8
2.3	Monodromy . . . . .	10
2.3.1	Classical Monodromy . . . . .	10
2.3.2	Quantum Monodromy . . . . .	10
2.3.3	Calculating Monodromy from the Energy-Momentum Map . .	12
2.4	Quasi-Exact Solvability . . . . .	12
<b>3</b>	<b>Results</b>	<b>14</b>
3.1	Monodromy of the Quadratic Pendulum . . . . .	14
3.2	Bidromy of the Corresponding Supersymmetric Partner Potentials . .	16
<b>4</b>	<b>Conclusion</b>	<b>20</b>

# Chapter 1

## Introduction

The quantum pendulum, i.e., a rigid rotor under a cosine potential and/or its variants, belongs to prototypical systems in quantum mechanics. It makes an appearance in a wide range of applications, in particular in molecular physics. Among these are manipulation of molecular rotation [1, 2, 3, 4, 5, 6, 7, 8, 9, 10, 11, 12, 13, 14, 15, 16, 17, 18, 19, 20, 21, 22, 23, 24, 25] and translation [26, 27], orbital imaging [28, 29, 30], deracemization [31], molecular trapping [32], quantum simulation [33, 34] and quantum computing [35, 36, 37, 38, 39, 40, 41].

A polar and polarizable molecule subject to electric and/or optical fields is the most common realization of the quantum pendulum. If the molecule is linear and its electronic angular momenta vanish (i.e., the molecule is in a  $^1\Sigma$  state), it is also the simplest one. Herein, we will concern ourselves with this simplest realization of the quantum pendulum. Its Hamiltonian is given by

$$H = B [\mathbf{J}^2 - \eta \cos \theta - \zeta \cos^2 \theta] \quad (1.1)$$

with  $B$  the rotational constant,  $\mathbf{J}^2$  the square of the angular momentum operator,  $\theta$  the polar angle between the molecular axis and the common direction of the electrostatic,  $\varepsilon_S$ , and optical,  $\varepsilon_L$ , field vectors, and  $\eta$  and  $\zeta$  the orienting and aligning dimensionless interaction parameters. Figure 1.1 illustrates the meaning of the above vectors and angles and provides a definition of the moment of inertia  $I$ , which is related to the rotational constant via  $B = \frac{\hbar^2}{2I}$ . The interaction parameters are then  $\eta = \frac{\mu \varepsilon_S}{B}$  for the orienting interaction and  $\zeta = \frac{(\alpha_{\parallel} - \alpha_{\perp}) \varepsilon_L^2}{2B}$  for the aligning interaction. An overview of values of  $\eta$  and  $\zeta$  for experimentally achievable field strengths and different molecules may be found in Table B1 of Ref. [42] by Sharma and Friedrich.

A general solution of the pendular eigenproblem – i.e., the eigenproblem for Hamiltonian (1.1) – can only be found by a numerical diagonalization of the corresponding truncated infinite-dimensional Hamiltonian matrix. Its matrix elements, which depend solely on the interaction parameters  $\eta$  and  $\zeta$ , can be obtained analytically in the free-rotor basis set,  $|j, m\rangle$ .

Previous work on the supersymmetry of the quantum pendulum [43] has revealed that the pendular eigenproblem does have analytic solutions, but only for a particular class of states (i.e., for stretched states) and a particular ratio of the interaction parameters such that  $k \equiv \frac{\eta}{2\sqrt{\zeta}}$  be an integer.

Follow-up work [44] has led to the realization that the pendular eigenenergy surfaces  $E = E(\eta, \zeta)$  exhibit (avoided) intersections, whose loci are given by integer

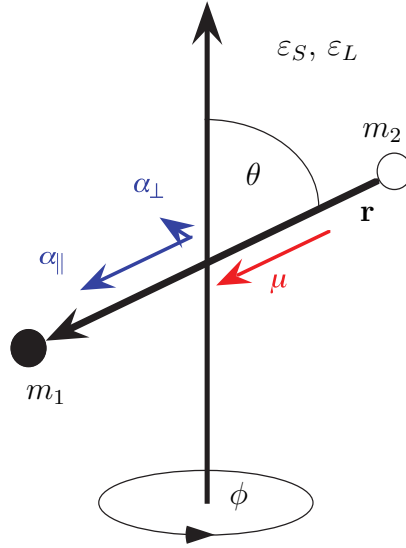


Figure 1.1: The static field  $\varepsilon_S$  interacts with the body-fixed dipole moment  $\mu$ , the optical field  $\varepsilon_L$  with the body-fixed static-polarizability components  $\alpha_\perp$  and  $\alpha_\parallel$  of the linear molecule. Also depicted are the polar angle  $\theta$  and azimuthal angle  $\phi$ , the molecular axis  $\mathbf{r}$ , as well as the atomic masses  $m_1, m_2$ . The molecule's moment of inertia is  $I = mr^2$  with reduced mass  $m = \frac{m_1 m_2}{m_1 + m_2}$  and  $r = |\mathbf{r}|$ .

values of  $k$ , termed from now on the *topological index*. Thus the condition for analytic solvability has been found to coincide with the equation for the intersection loci of the eigenenergy surfaces.

This curious coincidence is the main motivation for the analysis put forward in this thesis. If a more general relationship between this quasi-exact solvability and partial degeneracy of the spectrum of energy-eigenvalues could be established, it might provide a useful tool for determining either property in similar systems.

Classically, Hamiltonian (1.1) amounts to a completely integrable system with  $n$  degrees of freedom. That is to say, it possesses  $n$  independent integrals of motion  $F_i$  ( $i = 1, \dots, n$ ), which are mutually Poisson-commuting. As such, classically, it is exactly solvable, that is to say its trajectories can be obtained by *quadratures*.

However, integrability of the classical system does not imply exact solvability of the corresponding quantum mechanical system, as the latter is only solvable for a particular choice of  $\eta$  and  $\zeta$ .

The avoided crossings at integer  $k$  do, of course, amount to a quasi-degeneracy of the energy spectrum and thus characteristic changes in the structure of the systems energy-momentum map. The latter bears a close connection to the system's monodromy. The question of monodromy is that of the existence of a single consistent global assignment of quantum numbers, or — in the classical case — action-angle variables and as such might offer some insight into the quasi-exact solvability of the problem. The monodromy of the system can in turn be computed by analyzing its energy-momentum-map  $(E, m)$ , where  $E$  is the systems energy and  $m$  the projection quantum number corresponding classically to the azimuthal angular momentum  $p_\phi$ .

It has been shown in Ref. [44] that in the free-rotor ( $\eta, \zeta \rightarrow 0$ ) and harmonic-librator ( $\eta \rightarrow \infty$ ) limit the system is exactly solvable. The corresponding systems then exhibit trivial monodromy.

# Chapter 2

## Theoretical Foundations

### 2.1 Classically Integrable Systems and Action-Angle Coordinates

A Hamiltonian system of  $n$  degrees of freedom spanning a  $2n$ -dimensional phase space  $\Phi$ , is called *integrable* [45] if there exist  $n$  independent, mutually Poisson commuting integrals of motion  $F_k$  and a Hamiltonian  $\mathcal{H} = \mathcal{H}(F_1, \dots, F_n)$  such that

$$\{F_k, \mathcal{H}\} = \sum_{i=1}^n \frac{\partial F_k}{\partial q_i} \frac{\partial \mathcal{H}}{\partial p_i} - \frac{\partial F_k}{\partial p_i} \frac{\partial \mathcal{H}}{\partial q_i} = 0 = \frac{dF_k}{dt}, \quad k = 1, \dots, n. \quad (2.1)$$

Poisson commuting means that the  $F_i$  satisfy the relation

$$\{F_i, F_j\} = 0. \quad (2.2)$$

While integrable systems are rare among all possible Hamiltonian systems, they are of particular interest to mathematicians and physicists alike, as Hamiltonian systems which are explicitly solvable using the methods of traditional mathematical physics are invariably integrable [45, 46].

The question arises, what characteristics of integrable systems differentiate them from others, and how these relate to their solvability. The Louville-Arnol'd theorem [47] gives surprising insight into this matter. A complete analysis of its consequences can be found in Ref. [45].

#### 2.1.1 Proof of Integrability of the Classical Quadratic Pendulum

It can be shown easily that the quadratic pendulum, see Eq. (2.3) below, is integrable, by simply verifying Eqs. (2.1) and (2.2) with respect to the system's known integrals of motion, i.e. the azimuthal angular momentum  $p_\varphi$  and energy  $E$ . The classical Hamiltonian  $\mathcal{H}$  can be obtained by replacing  $\mathbf{J}^2$  with its classical analog, the rotational energy divided by the rotational constant, to find

$$\mathcal{H} = B \left( p_\theta^2 + \frac{p_\varphi^2}{\sin^2 \theta} - \eta \cos \theta - \zeta \cos^2 \theta \right). \quad (2.3)$$

The fact that  $p_\varphi$  and  $\mathcal{H}$  are in fact time invariant, i.e. integrals of motion, and thus satisfy Eq. (2.1) is trivial in the case of  $\mathcal{H}$ . For  $p_\varphi$  this can be shown by making

use of Hamilton's equations to verify that

$$\frac{dp_\varphi}{dt} = \frac{\partial \mathcal{H}}{\partial \varphi} = 0, \quad (2.4)$$

for  $\mathcal{H}$  is not explicitly dependent on  $\varphi$ .

The Poisson bracket of  $p_\varphi$  and  $\mathcal{H}$  also vanishes, as is evident from Eq. (2.4) and the linear independence of  $\theta$ ,  $\varphi$ ,  $p_\theta$  and  $p_\varphi$ .

$$\{\mathcal{H}, p_\varphi\} = \frac{\partial \mathcal{H}}{\partial \varphi} \frac{\partial p_\varphi}{\partial p_\varphi} - \frac{\partial \mathcal{H}}{\partial p_\varphi} \frac{\partial p_\varphi}{\partial \varphi} + \frac{\partial \mathcal{H}}{\partial \theta} \frac{\partial p_\varphi}{\partial p_\theta} - \frac{\partial \mathcal{H}}{\partial p_\theta} \frac{\partial p_\varphi}{\partial \theta} = 0 \quad (2.5)$$

Now it only remains to be shown that  $\mathcal{H}$  and  $p_\varphi$  are independent. This is to say, that their gradient vectors

$$\nabla p_\varphi = (0, 0, 0, 1) \quad (2.6)$$

$$\nabla \mathcal{H} = \left( -\frac{2p_\varphi^2}{\sin^3 \theta} \cos \theta + \eta \sin \theta + \zeta \cos \theta \sin \theta, 0, 2p_\theta, \frac{2p_\varphi}{\sin^2 \theta} \right) \quad (2.7)$$

with  $\nabla = (\partial \theta, \partial \varphi, \partial p_\theta, \partial p_\varphi)$ , are linearly independent.

For general  $\eta$  and  $\zeta$ , this is only the case, for

$$2p_\varphi^2 \cos \theta - \eta \sin^4 \theta - \zeta \cos \theta \sin^4 \theta = 0, \quad p_\theta = 0, \quad 0 < \theta < \pi, \quad (2.8)$$

corresponding to the parametric solutions

$$E_\pm(p_\varphi) = (\mathcal{H}_\pm(\theta), p_\varphi(\theta)) = \left( \frac{1}{2}(\eta + \zeta) \sin \theta \tan \theta - \eta \cos \theta - \zeta \cos \theta, \pm \frac{\sqrt{\eta + \zeta}}{\sqrt{2} \sqrt{\cot \theta} \csc^{\frac{3}{2}} \theta} \right), \theta \in [0, \pi] \setminus 0 \quad (2.9)$$

a plot of which is shown in Fig. 2.1.

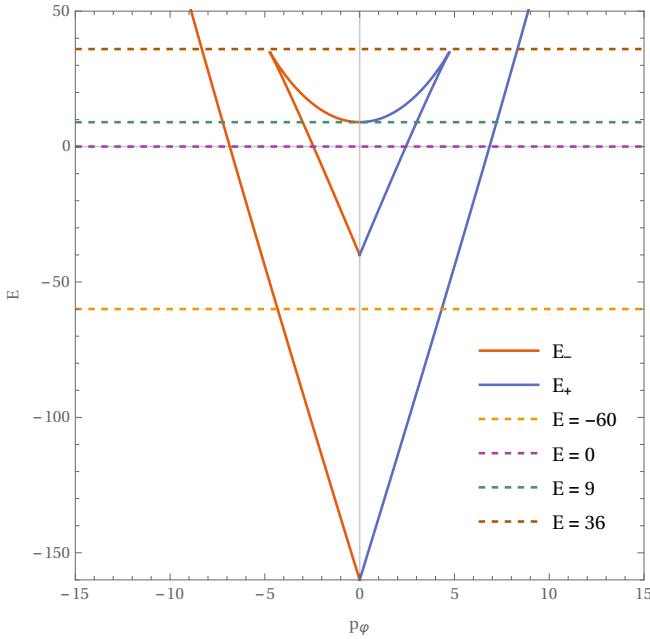


Figure 2.1: Critical values  $E_\pm$  of  $\mathcal{H}$  for  $\eta = 60$  and  $\zeta = 100$ . Energies used in in Fig.2.3 are marked with dashed lines.

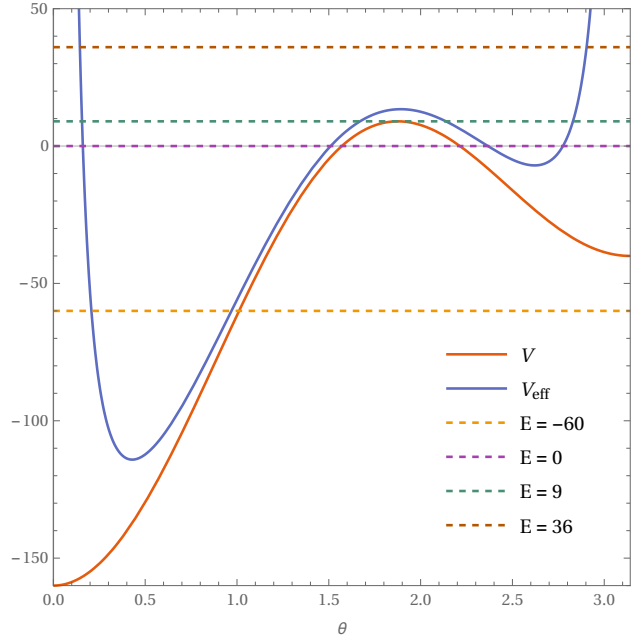


Figure 2.2: The potential  $V$  and effective potential  $V_{eff} = \frac{m^2}{\sin^2 \theta} - \eta \cos \theta - \zeta \cos^2 \theta$  for  $\eta = 60$ ,  $\zeta = 100$  and  $m = 2$ .

These are the critical values of the system, which correspond to the equilibria of the effective potential  $V_{eff}$ . As can be seen in a plot of  $V_{eff}$  in Fig. 2.2, three such equilibria exist. The global minimum naturally corresponds to the lowest critical line in Fig. 2.1, the local minimum corresponds to the critical line above it and the unstable equilibrium corresponds to the curved critical line  $[\alpha_+, \alpha_-]$ . The latter two meet at the points  $\alpha_+$  and  $\alpha_-$ , where the shallow well ceases to exist, as  $p_\varphi$  becomes larger.

### 2.1.2 The Liouville-Arnol'd Theorem

As shown above, the system possesses two integrals of motion  $\mathcal{H}$  and  $p_\varphi$ . These define its energy-momentum map

$$\mathcal{EM} : TS^2 \rightarrow \mathbb{R}^2 : \Phi \rightarrow (\mathcal{H}, p_\varphi) = (E, m) \quad (2.10)$$

It is instructive to regard the fibers  $\mathcal{M}_{E,m} = \mathcal{EM}^{-1}(E, m)$ , which are diffeomorphic to disjoint unions 2-Tori  $T^2$  in phase space  $\Phi$  according to the Liouville-Arnol'd theorem [47]. New coordinates  $\theta_1, \theta_2, I_1(\mathcal{H}, p_\varphi), I_2(\mathcal{H}, p_\varphi)$ , or *action-angle variables* can be introduced in a neighborhood of these tori by means of a canonical transformation, such that they evolve in time as

$$I_k(t) = I_k(0), \quad \theta_k = \omega_k(I)t + \theta(0), \quad \omega_k(I) = \frac{\partial \mathcal{H}}{\partial I_k}. \quad (2.11)$$

Hence, given a starting point  $\xi(0)$ , the time-evolved points  $\xi(t)$  on  $\mathcal{M}_{E,m}$  are multiperiodic functions of the angles  $\theta_1, \theta_2$ , which can be obtained by *quadratures*, i.e. solving transformation equations and integrating known functions[45]. The theorems introduced here for 2 dimensions are also valid for n-dimensional systems.

### 2.1.3 Cusp Singular Points

For regular values of  $\mathcal{EM}$  the fibers  $\mathcal{M}_{E,m}$  will be one (Fig. 2.3 a)) or two (Fig. 2.3 b)) smooth disjoint  $T^2$ , for energy regions with a single, or two potential wells present, respectively. For critical values of  $\mathcal{EM}$  however, the  $T^2$  will not be smooth but will carry a distinct signature of the critical values, to which they correspond. For the curved line of hyperbolic critical values  $[\alpha_+, \alpha_-]$  [48], the  $\mathcal{M}_{E,m}$  take the form of cuspidal tori (Fig.2.3 c)), or bitory (Fig.2.3 d)), as can be seen from the bisections of these tori in Fig. 2.4. These cusp singularities are obstructions to a smooth variation of action-angle variables as is required for our analysis in Sec.2.3.3.



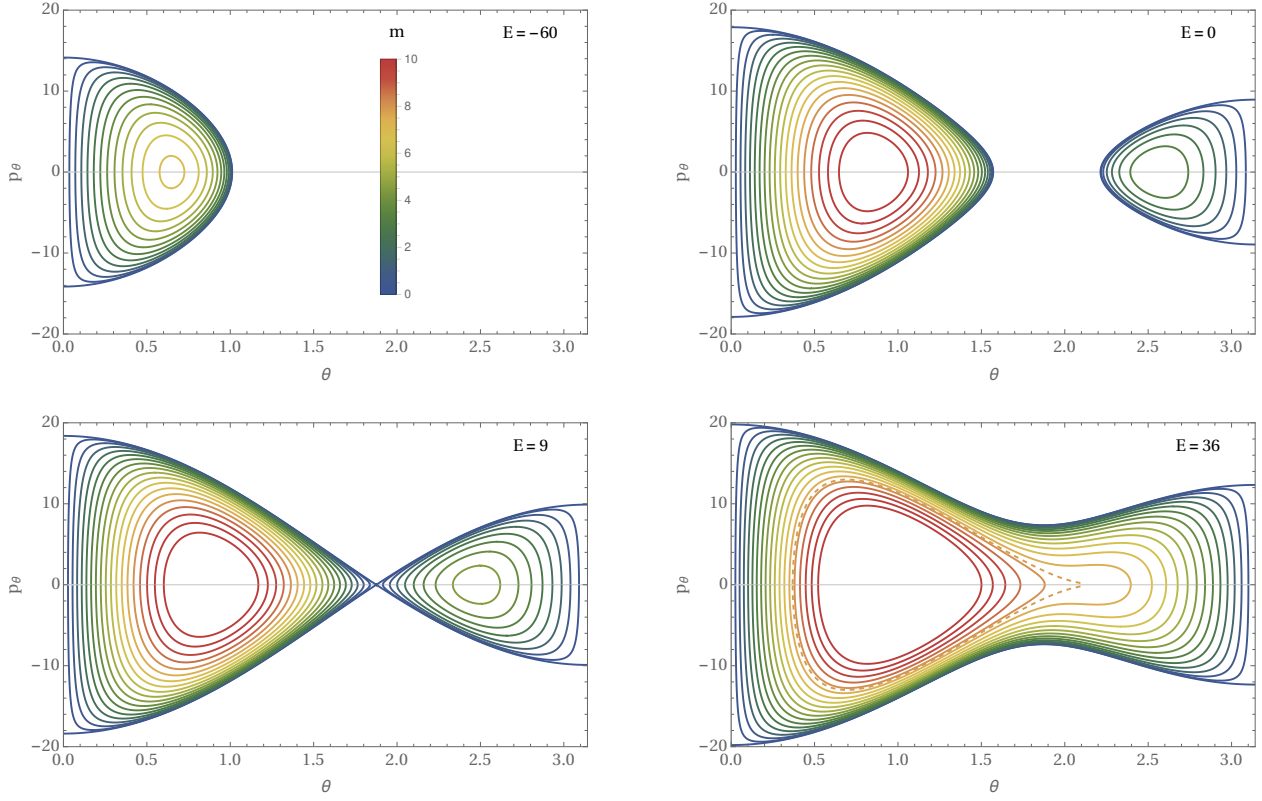


Figure 2.3: Sections of tori  $\mathcal{M}_{E,m}$ , i.e. the graphs of  $p_\theta(\theta)$ , for a range of  $m$  and four different Energies  $E$  (depicted in Fig. 2.2). The dashed line in  $E = 36$  corresponds to a cuspidal torus.

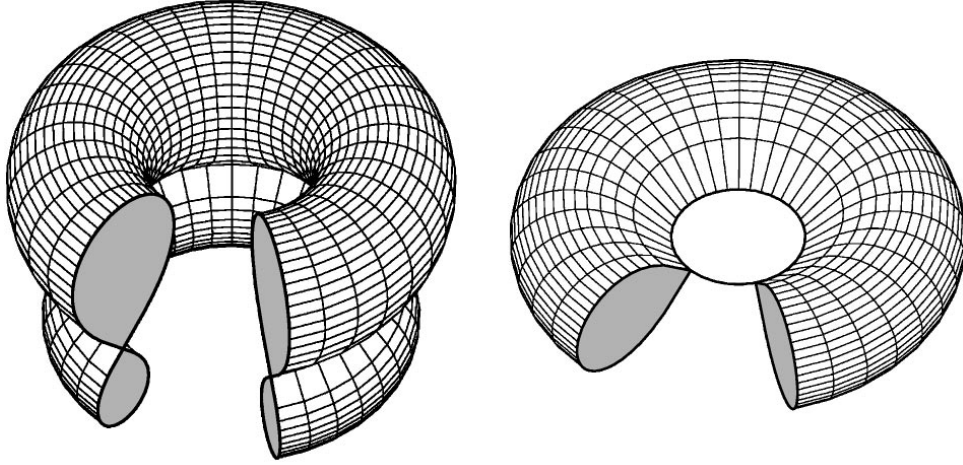


Figure 2.4:  $\mathcal{M}_{E,m}$  of hyperbolic critical values are pinched tori, i.e cuspidal tori or bitori. This figure was taken from [49]

It is important to note that  $\mathcal{EM}$  has two leaves, which are connected at the line of hyperbolic critical values. The smaller leaf  $A'$  represents states, which are localized within the shallow well and the larger leaf  $A$  represents states localized in the deeper well, as well as delocalized states. The two leaves overlap, of course for all values of  $\mathcal{EM}$  for which  $\mathcal{M}_{E,m}$  are two disjoint tori, which is the whole region covered by  $A'$ . Understanding the nature of the  $\mathcal{M}_{E,m}$  at the critical lines is vital to choosing the right paths for analysis in Sec. 3.

## 2.2 The Quantum Pendulum

The quantum counterpart of the classical system with Hamiltonian (1.1) is the main subject of this thesis. It bears the usual correspondance to the classical case, though it may be noted that the dynamics of the classical case depends solely on the dimensionless ratio  $\frac{\eta}{\zeta}$  [50] while the quantum dynamics also depends on the absolute values of  $\eta$  and  $\zeta$ , due to the presence of the fixed quantity  $\hbar$  in the rotational constant  $B$ .

### 2.2.1 The Eigenvalue Problem

The energy eigenvalues of our the quantum pendulum are readily computed by diagonalizing  $H$  in the free-rotor basis [44], the eigenfunctions of which are –apart from a normalization factor– spherical harmonics  $Y_j^m(\theta, \phi)$ . The resulting integrals  $\langle j', m' | H | j, m \rangle$  are easily evaluated analytically by making use of the "integral over the triple-product" theorem, (see e.g. Zare [51]), since the potential terms can also be written as linear combinations of spherical harmonics. The orienting interaction can thus be recast as

$$-\eta \cos \theta = -\eta \sqrt{\frac{4\pi}{3}} Y_1^0(\theta, \phi) \quad (2.12)$$

and the aligning interaction as

$$-\zeta \cos^2 \theta = -\zeta \frac{4}{3} \sqrt{\frac{\pi}{5}} Y_2^0(\theta, \phi) + \sqrt{\frac{5}{4}} Y_0^0(\theta, \phi). \quad (2.13)$$

As for all rotating bodies, the matrix elements of the rotational energy, i.e. the squared angular momentum operator are

$$\langle j', m' | \mathbf{J}^2 | j, m \rangle = j(j+1) \delta_{j',j} \delta_{m',m}. \quad (2.14)$$

It should be noted that the eigenstates of  $H$  have indefinite parity, as the  $\cos \theta$  operator changes parity, while the  $\mathbf{J}^2$  and  $\cos^2 \theta$  operators preserve parity.

The matrix elements for the orienting interaction are now simply integrals over three spherical harmonics with the respective coefficients of Eqs. (2.12) and (2.13) and the free-rotor eigenfunctions and are given by

$$\begin{aligned} \langle j', m' | -\eta \cos \theta | j, m \rangle &= -\eta \left[ \frac{(j+m)(j-m)}{(2j+1)(2j-1)} \right]^{\frac{1}{2}} \delta_{j',j-1} \delta_{m',m} \\ &\quad - \eta \left[ \frac{(j+m+1)(j-m+1)}{(2j+3)(2j+1)} \right]^{\frac{1}{2}} \delta_{j',j+1} \delta_{m',m}. \end{aligned} \quad (2.15)$$

Similarly, the matrix elements of the aligning interaction are given by

$$\begin{aligned} \langle j', m' | -\zeta \cos^2 \theta | j, m \rangle &= -\zeta \left[ \frac{1}{3} + \frac{2(2j+1)[j(j+1)-3m^2]}{3(2j+3)(2j+1)(2j-1)} \right] \delta_{j',j} \delta_{m',m} \\ &\quad - \zeta \left[ \frac{(j+m)(j+m-1)(j-m)(j-m-1)}{(2j-1)^2(2j+1)(2j-3)} \right]^{\frac{1}{2}} \delta_{j',j-2} \delta_{m',m} \\ &\quad - \zeta \left[ \frac{(j+m+2)(j+m+1)(j-m+2)(j-m+1)}{(2j+3)^2(2j+5)(2j+1)} \right]^{\frac{1}{2}} \delta_{j',j+2} \delta_{m',m}. \end{aligned} \quad (2.16)$$

Due to the linearity of  $\langle j', m' | \cdot | j, m \rangle$ , the complete Hamiltonian can thus be recast as the sum of (2.14), (2.15) and (2.16). The resulting matrix was easily computed in a sufficiently large dimension  $N$  using Wolfram *Mathematica*10.0 and then diagonalized with *Matlab*'s 'Eig' function. Each matrix-diagonalization then provides  $N$  eigenvalues.

## 2.2.2 The Quantum Energy-Momentum Map

In correspondence to the classical case the energy-momentum map  $EM = (H, m)$  of the quantum system can now be constructed by simply plotting the energy eigenvalues  $E_{j,m}$  against the good quantum number  $m$ , i.e. the projection of the angular momentum on the space fixed axis, as for example in Fig. 3.2. The resulting map is the basis for the analysis put forward in Sec. 2.3.3.

## 2.2.3 An Analysis of Numerical Errors

Our numerical method to calculate the eigenvalues is, of course, of varying precision. Generally it is to be expected that the results will become less precise with increasing quantum number  $J$ . The errors also depend on the values of the interaction parameters  $\eta$  and  $\zeta$ .

A simple empirical analysis of these errors can give sufficient insight into the precision of our data before we draw conclusions from them. To this end we generated sets of eigenvalues  $E_{J,m}^N$  with equal parameters, save the dimension  $N$  of the truncated Hamiltonian matrices that were used for their generation. We then calculated absolute errors  $u_N = |E_{J,m}^N - E_{J,m}^{N_{max}}|$  of each eigenvalue  $E_{J,m}^N$ , where  $E_{J,m}^{N_{max}}$  is the corresponding eigenvalue of highest precision. By checking for convergence we can state a good estimate for each  $u_N$  and an upper bound for the remaining uncertainty  $u_{J,m}^{N_{max}}$ . In all analyzed cases,  $u_{J,m}^N$  converged quickly and uniformly upto a value of  $u_{J,m}^N \approx 10^{-12}$ , which is certainly sufficient for the analysis of monodromy put forward in Sec. 3.

It can be seen in Fig. 2.5–2.7 that, with increasing interaction parameters  $\eta$  and  $\zeta$ , larger  $N$  are required to achieve a desired precision.

For the relatively low and experimentally achievable [42]  $\eta = 20, \zeta = 100$ , the empirical relation  $u_{J,m}^{J+10} \approx 10^{-(3+0.25J)}$  might be inferred from the results in Fig. 2.5, but is naturally of limited scope and fails as the maximal precision is approached. In any case errors of  $u_{J,m}^N \approx 10^{-12}$  are achieved at  $N = J + 10$  for  $J > 40$  and  $N = J + 20$  for all  $J$ .

The larger interaction parameters  $\eta = 175$  and  $\zeta = 430$  of Fig. 2.6 mandate larger  $N$  to achieve comparable precision. Again  $u_{J,m}^{J+10} \approx 10^{-(0.06J)}$  may be used as a very rough estimate, however this relation fails for  $J < 30$ . Still a minimal error of  $u_{J,m}^{J+10} \approx 10^{-12}$  is achieved at  $N = J + 20$  for  $J > 60$  and at  $N = J + 35$  for all  $J$ .

For the somewhat unrealistically large interaction parameters  $\eta = 400, \zeta = 1600$  much larger  $N$  are required (see Fig. 2.7). Here only at  $N = J + 45$ ,  $J > 50$  minimal precision of  $u_{J,m}^{J+10} \approx 10^{-12}$  is achieved and only at  $N = J + 50$  is it achieved for all

$J$ . In Fig.2.8 an energy-momentum map of  $H$  (1.1) is also displayed with a broad scope of  $J$ , to give some overview over the precision of our method. It can be seen here that the topmost energy levels  $E_{j,m}$  are noticeably irregular, while the errors of all other  $E_{j,m}$  are negligibly small in terms of determining the structure of  $EM$ .

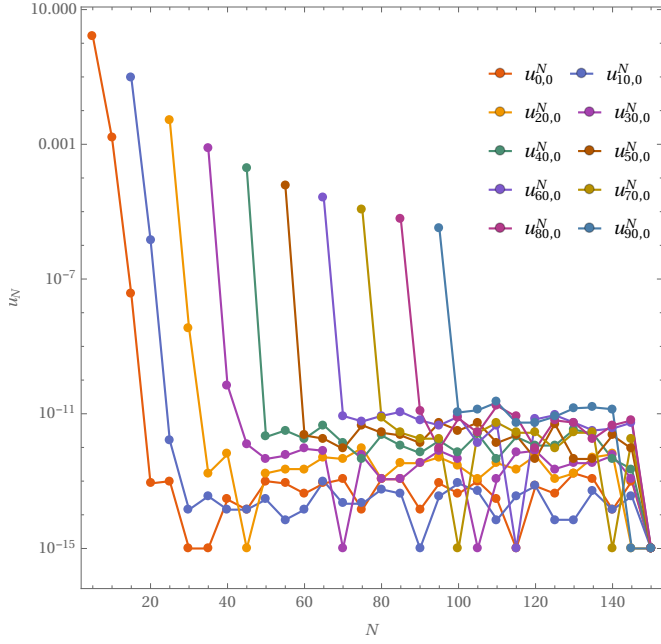


Figure 2.5: Absolute errors  $u_N$  for  $\eta = 20$ ,  $\zeta = 100$ . For a number of energy levels  $E_{j,m}$  at  $m = 0$ .

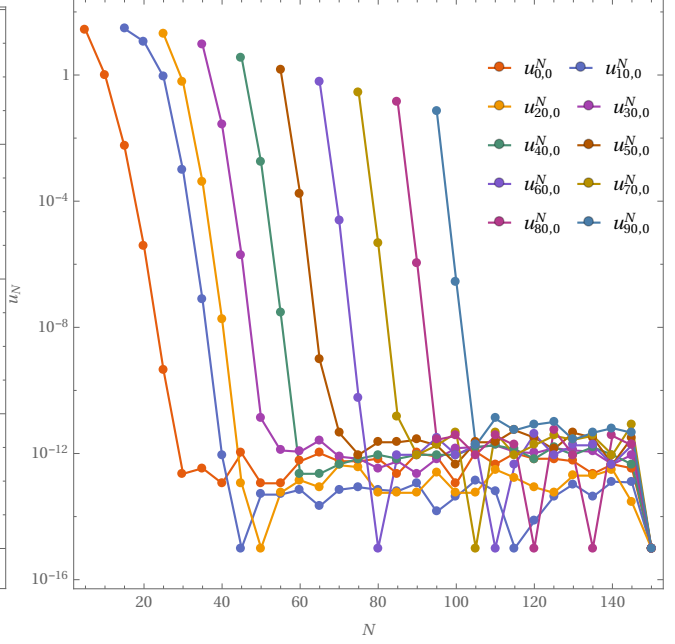


Figure 2.6:  $u_N$  for  $\eta = 175$ ,  $\zeta = 430$ . It should be noted that for each  $u_{j,m}^N$  the lowest dimension displayed is  $N = J + 5$ .

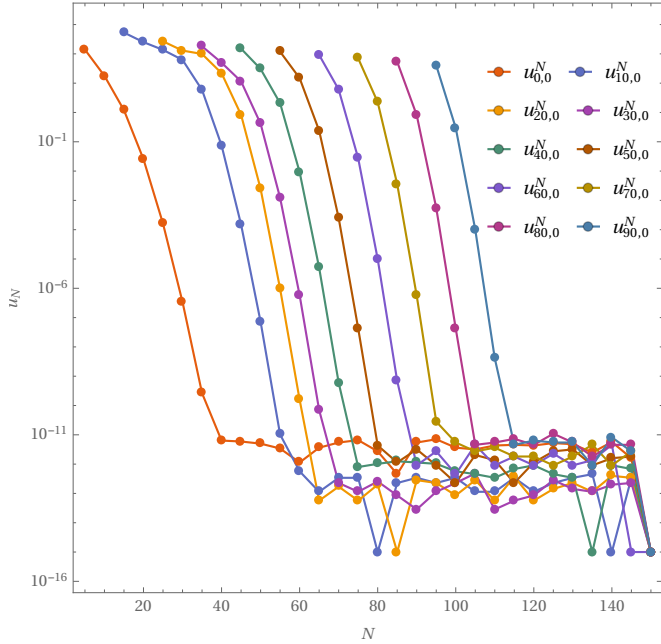


Figure 2.7: Absolute errors  $u_N$  for  $\eta = 400$ ,  $\zeta = 1600$ .

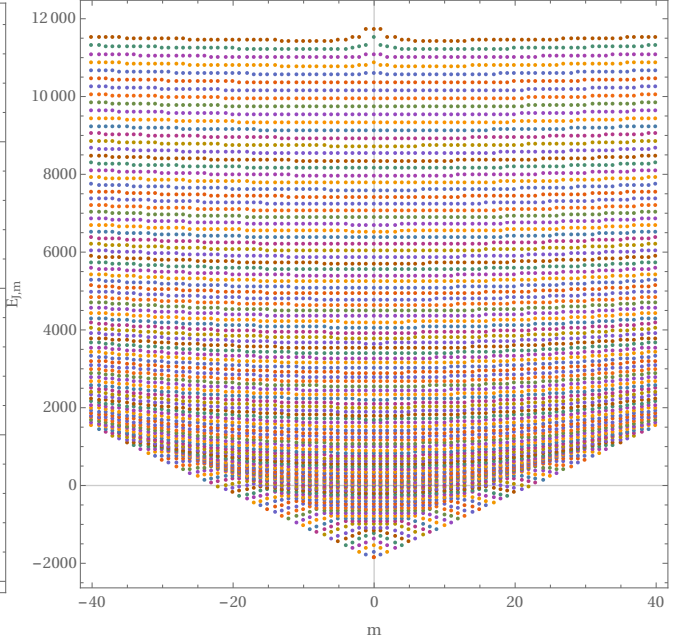


Figure 2.8: Energy-momentum map of  $H$  (1.1) for  $\eta = 400$ ,  $\zeta = 1600$ ,  $N = 150$  and  $J = 0, \dots, 150$ .

## 2.3 Monodromy

### 2.3.1 Classical Monodromy

As stated in Sec. 2.1.2, it is possible to construct smooth action-angle variables in a neighborhood of each  $\mathcal{M}_{E,m}$ , which is a smooth torus  $T^2$ . The question arises, as to whether it is also possible to assign *global* action angle variables, i.e. continuously expand the local coordinate system to the system's entire phase space. This is the question of the system's monodromy. As the choice of action-angle variables is not unique, the answer to this question is not always trivial.

#### Cusp singularities and topology of fiber bundles

The  $T^2$  bundle over a circle  $\Gamma$ , which loops around a cusp singularity  $\alpha$  of the energy-momentum map  $\mathcal{EM}$  is non-trivial [52], i.e.  $\mathcal{M}_\Gamma$  is not diffeomorphic to  $T^2 \times S_1$ . Because of this the  $T^2$  in a neighborhood of the pinched Torus  $\mathcal{EM}^{-1}(\alpha)$  cannot be labeled uniquely and global action-angle variables cannot be introduced here [53, 54].

In contrast to this, it follows from the existence of global action-angle variables that the transport according to the smooth functions  $I_k$  of a torus around a closed loop in phase space must return all variables to their initial values. Any such loop does not contain isolated singularities and may thus be smoothly contracted into a point.

#### The classical period lattice

For a regular value  $f$  of  $\mathcal{EM}$  the Hamiltonian vector field

$$X_{F_i} = (\{q_i, F_i\}, \dots, \{q_k, F_i\}, \{p_i, F_i\}, \dots, \{p_k, F_i\}) \quad (2.17)$$

of the integral  $F_i$  defines a flow  $g_{F_i}$  on  $\mathcal{M}_f$ .

Classically the period lattice vectors on  $\mathcal{M}_f$  are defined as linear combinations of flows  $g_{F_i}$  required to mimic the  $2\pi$ -periodic flows  $g_{I_i}$ , generated by the actions  $I_i$  of (2.11). That is the matrix  $A_f$ , whose columns are the lattice vectors so that

$$\begin{pmatrix} g_{I_i} \\ \vdots \\ g_{I_n} \end{pmatrix} = A^\dagger \begin{pmatrix} g_{F_i} \\ \vdots \\ g_{F_n} \end{pmatrix}. \quad (2.18)$$

This lattice can be extended to an open small neighborhood  $D_f$  of  $f$ , given  $D_f$  also lies in the set of regular values [49, 45].

### 2.3.2 Quantum Monodromy

By analogy, the notion of monodromy in quantum mechanics is related to the existence of a global consistent assignment of quantum numbers. A system with non-trivial monodromy does not permit such an assignment in such a way that the extrapolation of quantum numbers  $\nu(E, m)$  happens in a smooth way, which is a necessary requirement for physically meaningful quantum numbers [49]. We can

use these insights to evaluate monodromy from the numerically generated energy-momentum map  $EM$ .

### The quantum period lattice and local quantum numbers

In our case, the quantum period lattice can be introduced in point  $(E, m)$  through the Einstein-Brillouin-Keller action quantization following the action-relation

$$I_k(E, m) = 2\pi\hbar(\nu_k + \mu_k), \quad \nu_k \in \mathbb{N}_0, \quad (2.19)$$

with local quantum numbers  $\nu_k$ , Maslov indexes  $\mu_k$  and actions  $I_k$  (2.11). The quantum numbers  $\nu_k$  and  $m$  then locally define the vectors of the period lattice (see Fig. 2.9). The lattice vectors in  $D_{E,m}$  can still be defined by local actions, which are smooth functions of the  $F_i$ . The actions and integrals will be referred to by their corresponding quantum operators in this paragraph, to clarify the relation to the quantum numbers.

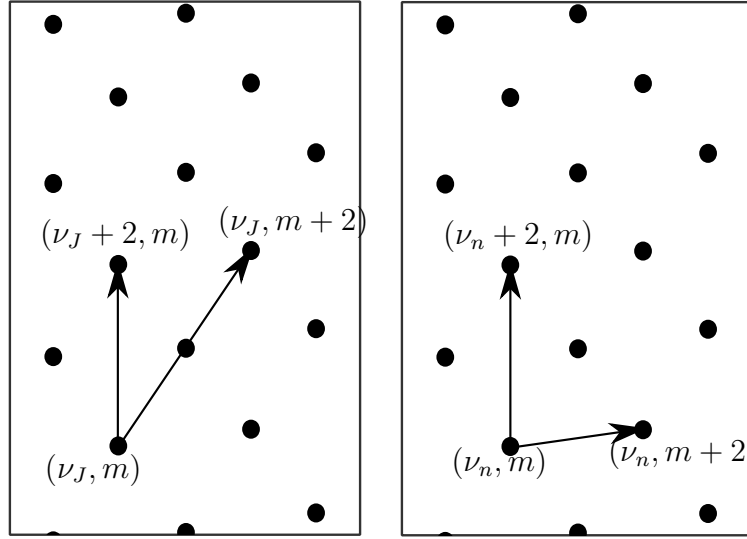


Figure 2.9: Two different choices of an elementary cell of the period lattice corresponding to the quantum numbers  $\nu_J = J$  and  $\nu_n = 2J - |m|$

One of the integrals of motion of the pendulum, the azimuthal angular momentum  $m$  already defines a periodic flow, while the other, the Hamiltonian  $H$  does not. To describe the period lattice for the whole of  $EM$  we may take an exemplary flow on a regular torus  $\mathcal{M}_{E,m}$  as in Fig. 2.10. We take a periodic orbit  $\Gamma$  of  $g_m$  on  $\mathcal{M}_f$ . We also take an orbit  $g_H$  starting at  $\xi_0 \in \Gamma$  and returning to  $\xi' \in \Gamma$  after *the period of first return*  $T_{E,m}$ .

We then see that the latter also induces a rotation  $\Theta$  along  $\Gamma$ . Hence, we find that, to satisfy (2.18), the lattice vectors must be

$$A_{E,m} = \frac{1}{2\pi} \begin{pmatrix} 2\pi & -\Theta_{E,m} \\ 0 & T_{E,m} \end{pmatrix}. \quad (2.20)$$



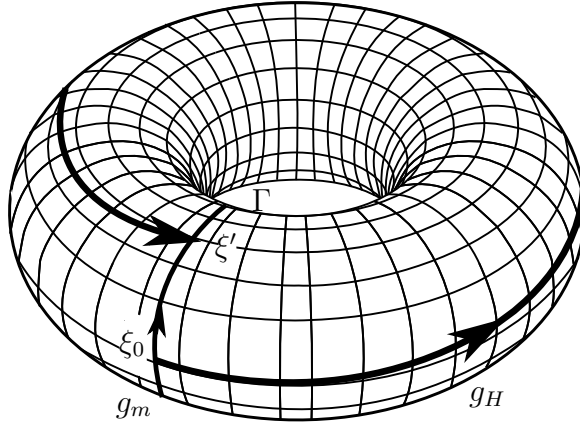


Figure 2.10: The flows of the vector fields  $X_m$  and  $X_H$ . Where  $g_m$  is periodic while  $g_H$  induces a rotation  $\Theta$  along  $X_{p_\varphi}$ .

### 2.3.3 Calculating Monodromy from the Energy-Momentum Map

In order to reveal the monodromy in our system, we will follow the method of analytic continuation of period lattices [49, 55, 45]. To this end, we follow a closed loop  $\gamma$  in the set of regular values around the critical line  $[\alpha_+, \alpha_-]$  and try to continue the period lattice of quantum states as defined by the quantum numbers  $\nu_k(k = n, J)$  (see. Fig 2.9) for consecutive values of  $(E, m) \in \gamma$ .

After completing this loop and returning to the initial point  $(E_1, m_1) = (E_0, m_0)$  we compare the corresponding lattice matrixes  $A_{E_1, m_1}$  and  $A_{E_0, m_0}$ . If the lattices do not coincide, so that the monodromy matrix  $M$  defined by

$$MA_{E_0, m_0} = A_{E_1, m_1} \quad (2.21)$$

is not a unit matrix, then the system has non-trivial monodromy and the actions used to define the period lattices are not global [49].

## 2.4 Quasi-Exact Solvability

While integrability and exact solvability coincide classically, this is not the case in quantum mechanics, due to the absence of a quantum analogue of the Liouville-Arnol'd theorem. [56]

In any case exactly solvable models, such as the hydrogen atom or the harmonic oscillator, are exceedingly rare in quantum physics. There do, however, also exist a larger number of quasi-exactly solvable models, which have been categorized in [57, 58] that have the characteristic property of only admitting analytic solutions for an arbitrarily large but finite part of the spectrum and only when the potential parameters satisfy a specified condition [59].

The quadratic pendulum (1.1) is quasi-exactly solvable for a certain choice of interaction parameters  $\eta$  and  $\zeta$  such that

$$\frac{\eta}{2\sqrt{\zeta}} = k, \quad k \in \mathbb{N}. \quad (2.22)$$

For these systems with integer  $k$ , the tunneling doublets degenerate as can be seen in Fig. 3.1, and some solutions can be found analytically. This fact has been put forward by Schmidt and Friedrich in Ref. [44], where some energy levels (ground states and first excited state) and the corresponding eigenfunctions have been found by means of the SUSY apparatus.



# Chapter 3

## Results

### 3.1 Monodromy of the Quadratic Pendulum

We compared the energy-momentum maps of two systems with integer (Fig. 3.1) and non-integer (Fig. 3.2) topological index  $k$ , computing the monodromy of both systems using the methods detailed in Sec. 2.3.3.

In full agreement with the theorems described in Sec. 2.3.1, we found that the system has monodromy. In particular its monodromy matrix is

$$M = \begin{pmatrix} 1 & 1 \\ 0 & 1 \end{pmatrix}, \quad (3.1)$$

as can be seen in Fig. 3.2 and Fig 3.1.

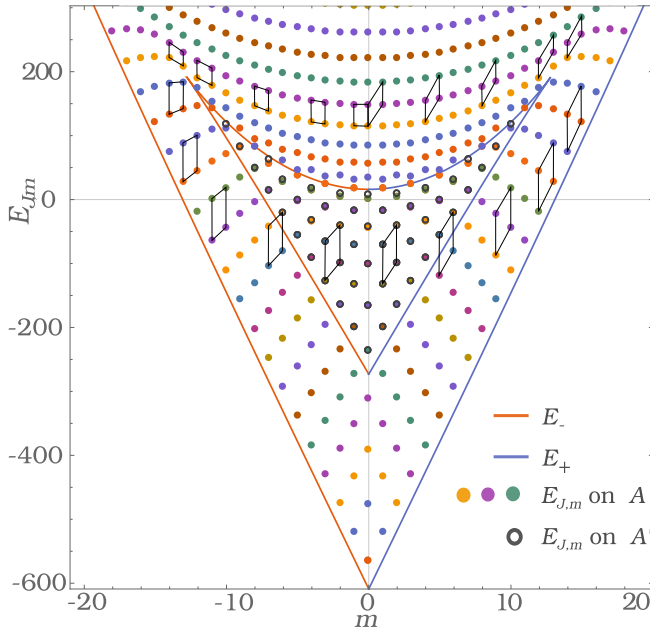


Figure 3.1:  $EM$  of  $H$  and critical lines (2.9) for  $\eta = 168$ ,  $\zeta = 441$ ,  $k = 4$ . Upper members of tunneling doublets are marked with grey circles. Colors correspond to equal rotational quantum number  $\nu_J$ .

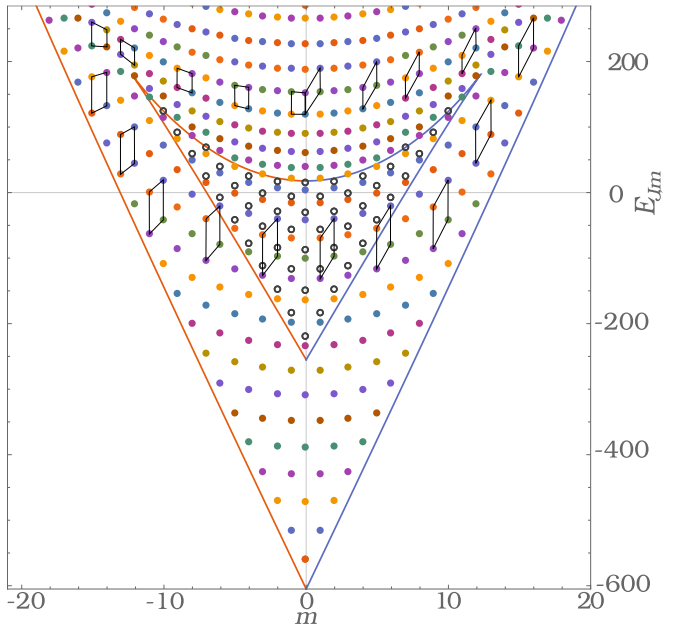


Figure 3.2:  $EM$  of  $H$  and critical lines (2.9) for  $\eta = 175$ ,  $\zeta = 430$ ,  $k = 4.22$ . Upper members of tunneling doublets are marked with grey circles. Colors correspond to equal librational quantum number  $\nu_n$ .

To illustrate this fact and shed some light on the qualitative consequences this has for the system, we also visualized a certain choice of quantum numbers that are locally smooth, i.e. define a smooth sequencing of states over certain domains of  $EM$  in Fig. 3.3. There exist two natural choices of such quantum numbers for our system. These are the librational quantum number  $\nu_n$  and the rotational quantum number  $\nu_J$  [52]. The librational quantum number  $\nu_n$  works best for small  $J$ , i.e strongly bound states, whose energy  $E_{j,m}$  resides in a low range for which the system is essentially a 1:1 resonant oscillator [49]. On the other hand  $\nu_J$  is smooth for large  $J$  and the corresponding range of high energies, where the system is similar to a free-rotor with a small perturbation. It can be seen in Fig. 3.3 that, together, these quantum numbers do indeed map the whole of  $A$  in a smooth manner.

As such, no difference exists in terms of monodromy between systems with integer and non-integer topological index  $k$ . Both systems exhibit non-trivial monodromy, as is mandated by the nature of the critical line  $[\alpha_+, \alpha_-]$ .

**Coinciding labels on  $A$  and  $A'$**  There is, however, a qualitative difference in the way these systems can be labeled, which is directly linked to the degeneracy of the tunneling doublets at interger  $k$ . If we introduce librational quantum numbers  $\nu'_n$  on the Leaf  $A'$  these are also smooth. However, for non-integer  $k$ ,  $\nu_n$  and  $\nu'_n$  and their corresponding classical actions cannot be smoothly connected to one-another and consequently we need three sets of quantum numbers to cover the whole of  $EM$  in this case.

For integer  $k$  on the other hand, such a connection is obviously possible as the energies of the  $\nu_n$ -polyads coincide and hence  $EM$  can be covered completely by only two labels. In particular, a single quantum number can be introduced to label  $A'$  and the corresponding region in  $A$ , which is peculiar, as these are disjoint domains of  $EM$ .

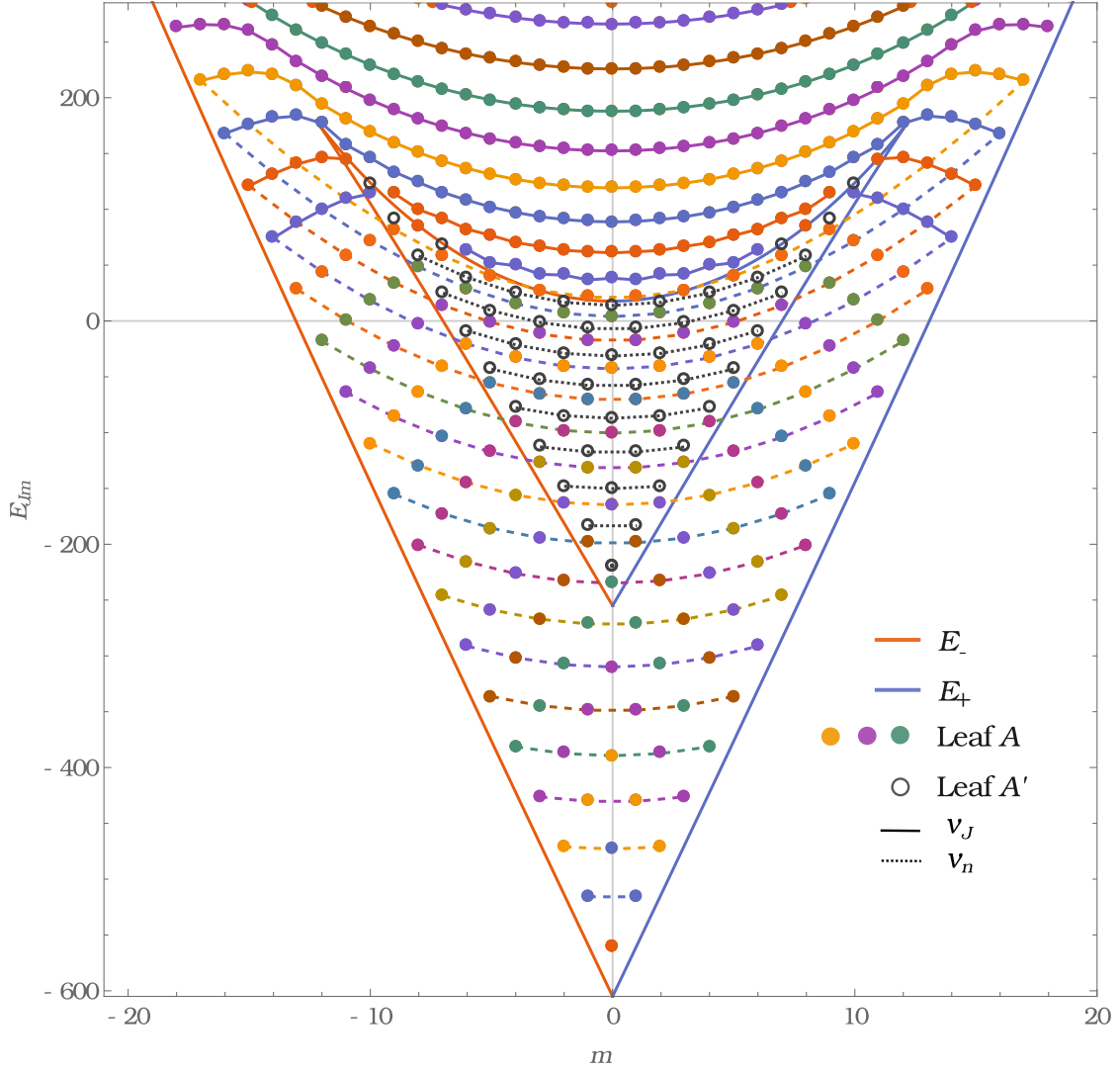


Figure 3.3:  $EM$  of  $H$  and critical lines (2.9) for  $\eta = 175$ ,  $\zeta = 430$ ,  $k = 4.22$ . States with equal  $\nu_J$  are connected with solid lines and states with equal  $\nu_n$  with dashed lines.

### 3.2 Bidromy of the Corresponding Supersymmetric Partner Potentials

As a complementary analysis, a similar approach was taken to analyse the case  $1_+$  partner potential

$$V_1^{1+} = \frac{m^2 - \frac{1}{4}}{\sin^2 \theta} - 2\beta(-m + 1) \cos \theta - \beta^2 \cos^2 \theta - 1/4, \quad (3.2)$$

which generally relates to the partner Hamiltonian  $H_1$  through

$$H_1 = \frac{\partial^2}{\partial \theta^2} + V_1 \quad (3.3)$$

and was used in the calculation of exact solutions in Ref. [44].

This system amounts to a swallowtail system [60] (see Fig. 3.7), as follows from the nature of the  $\mathcal{M}_{E,m}$  along the critical lines (corresponding to the dashed lines of Fig. 3.6) bordering the overlap region  $A_{\pm}$  of the energy-momentum map  $EM$ . On  $A_{\pm}$  the  $\mathcal{M}_{E,m}$  are two disjoint tori  $T_+^2 \cup T_-^2$ , one of which will degenerate into a circle  $S^1$  at either edge of  $A_{\pm}$  (see Fig. 3.4) defining the system to be of swallowtail form. We demonstrate this fact in Fig. 3.5, which shows cross sections of these  $\mathcal{M}_{E,m}$  for a range of different values of  $m$ .

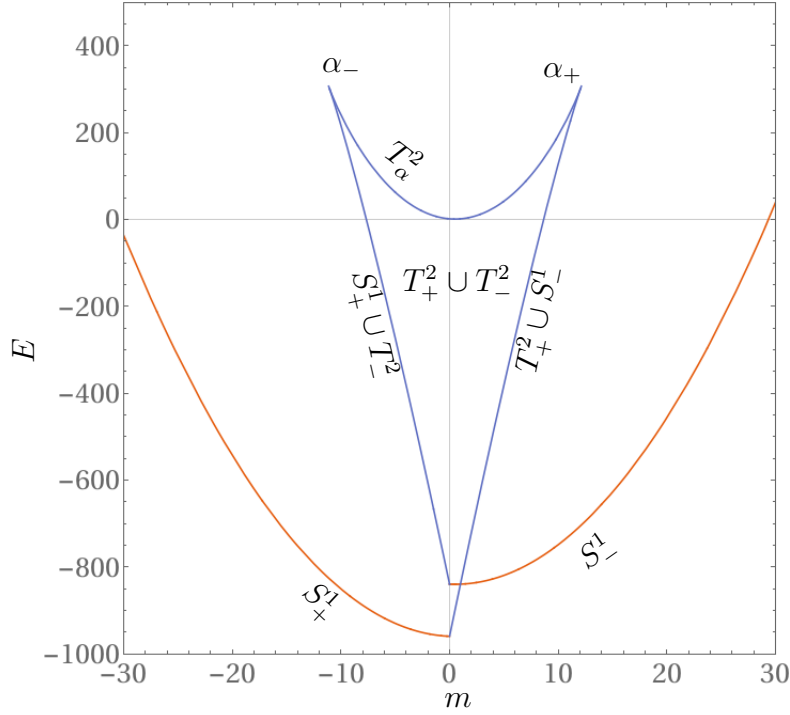


Figure 3.4: The critical lines  $E_{\pm}$  of the case  $1_+$  partner potential  $V_1$ . The topology of the corresponding  $\mathcal{M}_{E,m}$  is shown.  $T^2$  denote 2-tori  $S^1$  circles,  $T_{\alpha}^2$  cuspidal tori and the subscripts  $\pm$  denote whether the  $\mathcal{M}_{E,m}$  correspond to states localised around the global or local minimum of  $V_1^{1+}$ , i.e. if they lie on the upper or lower leaf of Fig. 3.6.

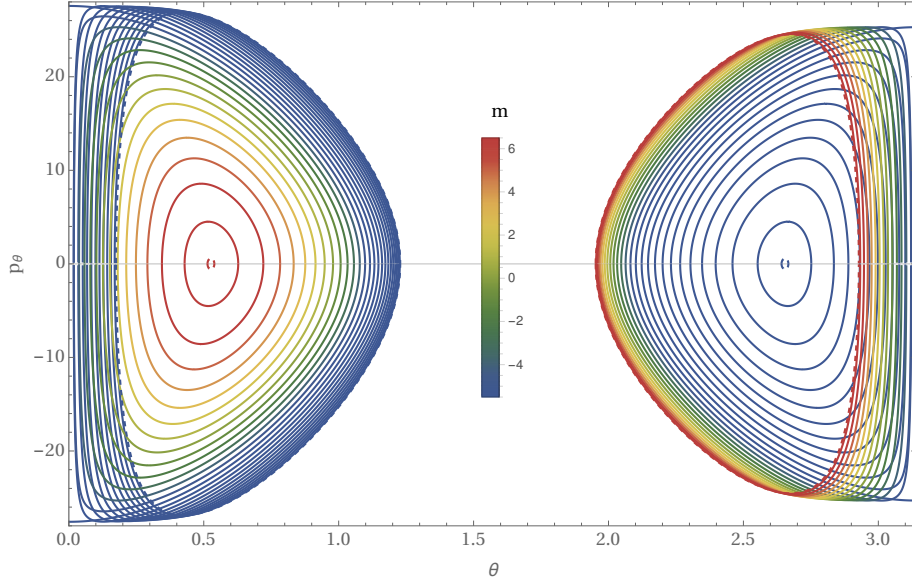


Figure 3.5: Cross sections of the  $\mathcal{M}_{E,m}$  corresponding to values within  $A_{\pm}$  for energy  $E = -200$ . It can be seen that at either critical line, the left or right graph contracts into a point, and thus the corresponding  $\mathcal{M}_{E,m}$  contracts into a circle. These cases are drawn with dashed lines.

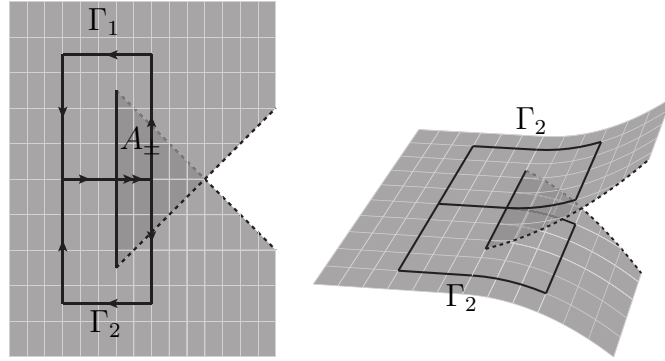


Figure 3.6: A schematic representation of the bifurcation diagram of the case  $1_+$  partner potential  $V_1^{1+}$ , depicting the bipath  $\Gamma_{1,2}$ . This figure was taken from [60] and relabeled.

Having determined the nature of our system's energy-momentum map we can now evaluate its bidromy following a similar approach to the one outlined in Sec. 2.3.3. To this end, we choose a "virtually closed"[61] bipath  $\Gamma_{1,2}$  (see Fig. 3.6), which is equivalent to the kind of closed path taken in Fig. 3.1 in terms of determining lattice changes. As depicted in Fig. 3.7, we transport an elementary cell along two closed loops  $\Gamma_1$  and  $\Gamma_2$  and compare the lattice vectors of the initial cell  $A_i$  and final cells  $A_f$  by adding up the latter two to combine lattice deformations along the loops  $\Gamma_1$  and  $\Gamma_2$ .

We find that this is effected by the transformation

$$A_f = \tilde{M}A_i = \begin{pmatrix} 1 & 1 \\ 0 & 2 \end{pmatrix} A_i \quad (3.4)$$

The system, thus, has bidromy.

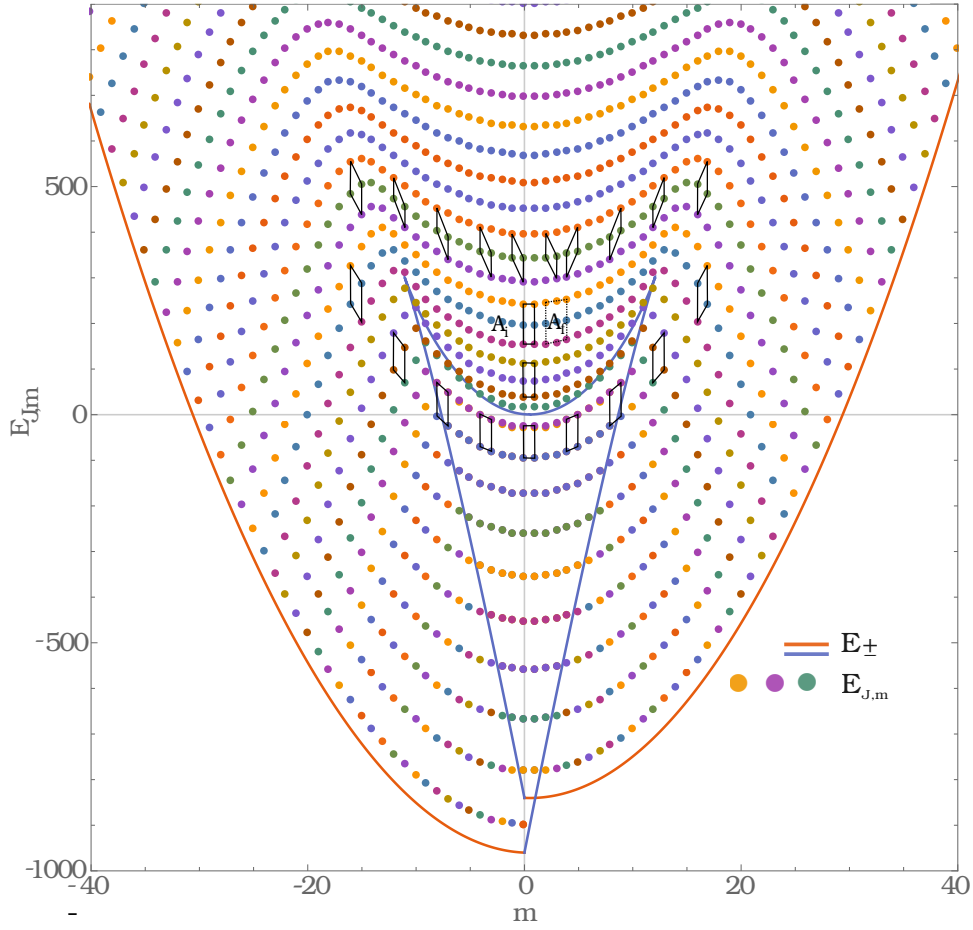


Figure 3.7:  $EM$  of the case  $1_+$  partner potential and critical lines (2.9) for  $\beta = 30$  and  $k = m - 1$ .

We analysed the case  $1_-$  partner potential  $V_1^{1-}$  in the same fashion as  $V_1^{1+}$  in Fig. 4.2 and found it to also have bidromy corresponding to the transformation

$$A_f = \tilde{M} A_i = \begin{pmatrix} 1 & 1 \\ 0 & 2 \end{pmatrix} A_i. \quad (3.5)$$

Finally, the case 2 partner potential  $V_1^2$  (see Fig. 4.1) was found to have Monodromy

$$M = \begin{pmatrix} 1 & 1 \\ 0 & 1 \end{pmatrix}, \quad (3.6)$$

as it is equivalent to the quadratic pendulum 1.1 for  $k = 1$ .

# Chapter 4

## Conclusion

The main result of this thesis is that choosing a ratio of the interaction parameters that satisfies the condition for quasi-exact solvability for the quantum pendulum problem does not affect the monodromy of the system. The monodromy matrix of the quadratic pendulum (1.1) was found to be

$$M = \begin{pmatrix} 1 & 1 \\ 0 & 1 \end{pmatrix} \quad (4.1)$$

for integer and non-integer  $k$  alike. Hence, monodromy is not a critical factor in determining whether the system will be quasi-exactly solvable or not. The monodromy matrix of the corresponding supersymmetric partner potential  $V_1^2$  is also  $M$  (4.1) as it is equivalent to the quadratic pendulum for  $k = 1$ .

We did, however, find a qualitative difference between quantum pendula with integer and non-integer  $k$  through our analysis of the energy-momentum map. For an integer  $k$  a qualitatively different labeling of the quantum states is possible, since labels on  $A$  and  $A'$  naturally coincide in this case as the tunneling doublets become degenerate. Hence the whole of  $EM$  can then be labeled by two quantum numbers.

The case  $1_+$  and case  $1_-$  partner potentials  $V_1^{1\pm}$  were both found to have bidromy, pertaining to the transformation

$$\tilde{M} = \begin{pmatrix} 1 & 1 \\ 0 & 2 \end{pmatrix}. \quad (4.2)$$

# Bibliography

- [1] SLENCZKA, Alkwin ; FRIEDRICH, B. ; HERSCHBACH, D.: Pendular alignment of paramagnetic molecules in uniform magnetic fields. In: *Phys. Rev. Lett.* 72 (1994), S. 1806
- [2] FRIEDRICH, B. ; SLENCZKA, A. ; HERSCHBACH, D.R.: Spectroscopy of pendular molecules in strong parallel electric and magnetic fields. In: *Can. J. Phys.* 72 (1994), S. 897
- [3] FRIEDRICH, Bretislav ; HERSCHBACH, Dudley: Enhanced orientation of polar molecules by combined electrostatic and nonresonant induced dipole forces. In: *J. Chem. Phys.* 111 (1999), S. 6157
- [4] FRIEDRICH, B. ; HERSCHBACH, D.: Manipulating Molecules via Combined Static and Laser Fields. In: *J. Phys. Chem. A* 103 (1999), S. 10280
- [5] ORTIGOSO, Juan ; RODRIGUES, Marta ; GUPTA, Manish ; FRIEDRICH, Bretislav: Time evolution of pendular states created by the interaction of molecular polarizability with a pulsed nonresonant laser field. In: *J. Chem. Phys.* 110 (1999), S. 3870
- [6] SEIDEMAN, Tamar: New means of spatially manipulating molecules with light. In: *J. Chem. Phys.* 111 (1999), S. 4397
- [7] SEIDEMAN, Tamar: Revival Structure of Aligned Rotational Wave Packets. In: *Phys. Rev. Lett.* 83 (1999), S. 4971
- [8] LARSEN, Jakob ; HALD, Kasper ; BJERRE, Nis ; STAPELFELDT, Henrik ; SEIDEMAN, Tamar: Three Dimensional Alignment of Molecules Using Elliptically Polarized Laser Fields. In: *Phys. Rev. Lett.* 85 (2000), S. 2470
- [9] CAI, Long ; MARANGO, Jotin ; FRIEDRICH, Bretislav: Time-Dependent Alignment and Orientation of Molecules in Combined Electrostatic and Pulsed Nonresonant Laser Fields. In: *Phys. Rev. Lett.* 86 (2001), S. 775
- [10] CAI, Long ; FRIEDRICH, Bretislav: Recurring molecular alignment induced by pulsed nonresonant laser fields. In: *Coll. Czech Chem. Commun.* 66 (2001), S. 991
- [11] AVERBUKH, Ilya ; ARVIEU, R: Angular Focusing, Squeezing, and Rainbow Formation in a Strongly Driven Quantum Rotor. In: *Phys. Rev. Lett.* 87 (2001), S. 163601
- [12] LEIBSCHER, Monika ; AVERBUKH, Ilya ; RABITZ, Herschel: Molecular Alignment by Trains of Short Laser Pulses. In: *Phys. Rev. Lett.* 90 (2003), S. 213001



- [13] SAKAI, Hirofumi ; MINEMOTO, Shinichirou ; NANJO, Hiroshi ; TANJI, Haruka ; SUZUKI, Takayuki: Controlling the Orientation of Polar Molecules with Combined Electrostatic and Pulsed, Nonresonant Laser Fields. In: *Phys. Rev. Lett.* 90 (2003), S. 83001
- [14] FRIEDRICH, Bretislav ; NAHLER, N. H. ; BUCK, Udo: The pseudo-first-order Stark effect and the orientation of HXeI molecules. In: *J. Mod. Opt.* 50 (2003), S. 2677
- [15] LEIBSCHER, Monika ; AVERBUKH, Ilya ; RABITZ, Herschel: Enhanced molecular alignment by short laser pulses. In: *Phys. Rev. A* 69 (2004), S. 13402
- [16] BUCK, Udo ; FÁRNÍK, Michal: Oriented xenon hydride molecules in the gas phase. In: *Int. Rev. Phys. Chem.* 25 (2006), S. 583
- [17] HÄRTELT, Marko ; FRIEDRICH, Bretislav: Directional states of symmetric-top molecules produced by combined static and radiative electric fields. In: *J. Chem. Phys.* 128 (2008), S. 224313
- [18] POTERYA, V. ; VOTAVA, O. ; FARNIK, M. ; ONCAK, M. ; SLAVICEK, P. ; BUCK, U. ; FRIEDRICH, B: In: *J. Chem. Phys.* 128 (2008), 104313 S.
- [19] LEIBSCHER, Monika ; SCHMIDT, Burkhard: Quantum dynamics of a plane pendulum. In: *Phys. Rev. A* 80 (2009), 12510. <http://dx.doi.org/10.1103/PhysRevA.80.012510>
- [20] HOLMEGAARD, Lotte ; NIELSEN, Jens H. ; NEVO, Iftach ; STAPELFELDT, Henrik: Laser-Induced Alignment and Orientation of Quantum-State-Selected Large Molecules. In: *Phys. Rev. Lett.* 102 (2009), S. 23001
- [21] OWSCHIMIKOW, Nina ; SCHMIDT, Burkhard ; SCHWENTNER, Nikolaus: State selection in nonresonantly excited wave packets by tuning from nonadiabatic to adiabatic interaction. In: *Phys. Rev. A* 80 (2009), S. 53409
- [22] OHSHIMA, Yasuhiro ; HASEGAWA, Hirokazu: Coherent rotational excitation by intense nonresonant laser fields. In: *Int. Rev. Phys. Chem.* 29 (2010), S. 619–663
- [23] GERSHNABEL, E. ; AVERBUKH, Ilya: Deflection of Field-Free Aligned Molecules. In: *Phys. Rev. Lett.* 104 (2010), S. 153001
- [24] OWSCHIMIKOW, Nina ; KÖNIGSMANN, F ; MAURER, J ; GIESE, Ph. ; OTT, A ; SCHMIDT, Burkhard ; SCHWENTNER, Nikolaus: Cross sections for rotational decoherence of perturbed nitrogen measured via decay of laser-induced alignment. In: *J. Chem. Phys.* 133 (2010), S. 044311
- [25] OWSCHIMIKOW, Nina ; SCHMIDT, Burkhard ; SCHWENTNER, Nikolaus: Laser-induced alignment and anti-alignment of rotationally excited molecules. In: *Phys. Chem. Chem. Phys.* 13 (2011), S. 8671
- [26] ZHAO, B.S. ; LEE, S.H. ; CHUNG, H.S. ; HWANG, S. ; KANG, W.K. ; FRIEDRICH, B. ; CHUNG, D.S.: Separation of a benzene and nitric oxide mixture by a molecule prism. In: *J. Chem. Phys.* 119 (2003), S. 8905

- [27] FILSINGER, Frank ; KÜPPER, Jochen ; MEIJER, Gerard ; HOLMEGAARD, Lotte ; NIELSEN, Jens H. ; NEVO, Iftach ; HANSEN, Jonas L. ; STAPELFELDT, Henrik: Quantum-state selection, alignment, and orientation of large molecules using static electric and laser fields. In: *J. Chem. Phys.* 131 (2009), S. 064309
- [28] ITATANI, J ; LEVESQUE, J ; ZEIDLER, D ; NIKURA, Hiromichi ; PÉPIN, H ; KIEFFER, J C. ; CORKUM, P B. ; VILLENEUVE, D M.: Tomographic imaging of molecular orbitals. In: *Nature* 432 (2004), S. 867
- [29] RUPENYAN, A. ; BERTRAND, J. B. ; VILLENEUVE, D. M. ; WÖRNER, H. J.: All-Optical Measurement of High-Harmonic Amplitudes and Phases in Aligned Molecules. In: *Phys. Rev. Lett.* 108 (2012), Jan, 033903. <http://dx.doi.org/10.1103/PhysRevLett.108.033903>. – DOI 10.1103/PhysRevLett.108.033903
- [30] MOHN, Fabian ; GROSS, Leo ; MOLL, Nikolaj ; MEYER, Gerhard: Imaging the charge distribution within a single molecule. In: *Nature Nanotech.* 07 (2012), S. 227
- [31] MADSEN, C. B. ; MADSEN, L. B. ; VIFTRUP, S. S. ; JOHANSSON, M. P. ; POULSEN, T. B. ; HOLMEGAARD, L. ; KUMARAPPAN, V. ; JÄYRGENSEN, K. A. ; STAPELFELDT, H.: A combined experimental and theoretical study on realizing and using laser controlled torsion of molecules. In: *The Journal of Chemical Physics* 130 (2009), Nr. 23. <http://dx.doi.org/http://dx.doi.org/10.1063/1.3149789>. – DOI <http://dx.doi.org/10.1063/1.3149789>
- [32] MEERAKKER, Sebastiaan Y T. d. ; BETHLEM, Hendrick L. ; VANHAECKE, Nicolas ; MEIJER, Gerard: Manipulation and Control of Molecular Beams. In: *Chem. Rev.* 112 (2012), S. 4828
- [33] MANMANA, Salvatore R. ; STAUDENMIRE, E. M. ; HAZZARD, Kaden R. A. ; REY, Ana M. ; GORSHKOV, Alexey V.: Topological phases in polar-molecule quantum magnets. In: *Physical Review B* 87 (2013), S. 081106 R
- [34] BARANOV, M. A. ; DALMONTE, M. ; PUPILLO, G. ; ZOLLER, P.: Condensed Matter Theory of Dipolar Quantum Gases. In: *Chem. Rev.* 112 (2012), S. 5012
- [35] ZHU, Jing ; KAIS, Sabre ; WEI, Qi ; HERSCHBACH, Dudley ; FRIEDRICH, Bretislav: Implementation of quantum logic gates using polar molecules in pendular states. In: *J. Chem. Phys.* 138 (2013), S. 024104. <http://dx.doi.org/10.1063/1.4774058>. – DOI 10.1063/1.4774058
- [36] WEI, Qi ; KAIS, Sabre ; FRIEDRICH, Bretislav ; HERSCHBACH, Dudley: Entanglement of polar molecules in pendular states. In: *J. Chem. Phys.* 134 (2011), S. 124107
- [37] WEI, Qi ; KAIS, Sabre ; FRIEDRICH, Bretislav ; HERSCHBACH, Dudley: Entanglement of polar symmetric top molecules as candidate qubits. In: *J. Chem. Phys.* 135 (2011), S. 154102
- [38] TROPFMANN, Ulrike ; TESCH, Carmen M. ; VIVIE-RIEDLE, Regina de: Preparation and addressability of molecular vibrational qubit states in the presence of anharmonic resonance. In: *Chem. Phys. Lett.* 378 (2003), S. 273

- [39] KORFF, B. M. R. ; TROPPEMANN, Ulrike ; KOMPA, K.-L. ; VIVIE-RIEDLE, Regina de: Manganese pentacarbonyl bromide as candidate for a molecular qubit system operated in the infrared regime. In: *J. Chem. Phys.* 123 (2005), S. 244509
- [40] SCHNEIDER, B.M.R. ; GOLLUB, C. ; KOMPA, K.-L. ; VIVIE-RIEDLE, Regina de: Robustness of quantum gates operating on the high frequency modes of  $\text{MnBr}(\text{CO})_5$ . In: *Chem. Phys.* 338 (2007), S. 291
- [41] DEMILLE, David: Quantum Computation with Trapped Polar Molecules. In: *Phys. Rev. Lett.* 88 (2002), S. 067901
- [42] SHARMA, Ketan ; FRIEDRICH, Bretislav: Directional properties of polar paramagnetic molecules subject to congruent electric, magnetic and optical fields. In: *New Journal of Physics* 17 (2015), Nr. 4, 045017. <http://stacks.iop.org/1367-2630/17/i=4/a=045017>
- [43] LEMESHKO, Mikhail ; MUSTAFA, Mustafa ; KAIS, Sabre ; FRIEDRICH, Bretislav: Supersymmetry identifies molecular Stark states whose eigenproperties can be obtained analytically. In: *New J. Phys.* 13 (2011), S. 063036
- [44] FRIEDRICH, Bretislav: Supersymmetry and eigensurface topology of the spherical quantum pendulum. In: *Physical Review A* 91 (2015)
- [45] LOWENSTEIN, John H.: *Essentials of Hamiltonian Dynamics*. Cambridge University Press, 2012
- [46] WHITTAKER, E. T.: *A Treatise on Analytical Dynamics of Particles and Rigid Bodies*. Cambridge University Press, 1988
- [47] *Mathematical Methods of Classical Mechanics*. Springer-Verlag, 1978
- [48] EFSTATHIOU, Konstantinos ; GIACOBBE, Andrea: The topology associated with cusp singular points. In: *Nonlinearity* 25 (2012), Nr. 12, 3409. <http://stacks.iop.org/0951-7715/25/i=12/a=3409>
- [49] K. EFSTATHIOU, D. A. S. M. Joyeux J. M. Joyeux: Global bending quantum number and the absence of monodromy in the  $\text{HCN} \leftrightarrow \text{CNH}$  molecule. In: *PHYSICAL REVIEW A* 69 (2004)
- [50] AL, C.A. A.: Quantum monodromy for diatomic molecules in combined electrostatic and pulsed nonresonant laser fields. In: *Chemical Physics Letters* 392 (2004), S. 486–492
- [51] *Angular Momentum: Understanding Spatial Aspects in Chemistry and Physics*. Jon Wiley & Sons, Inc., 1988
- [52] CHILD, Mark S.: Quantum Monodromy and Molecule Spectroscopy. In: *Advances in Chemical Physics* 136 (2007), S. 39–94
- [53] SCHLEIF, C.R. ; DELOS, J.B.: Monodromy and the structure of the energy spectrum of hydrogen in near perpendicular electric and magnetic fields. In: *Phys. Rev. A* (2007)

- [54] CUSHMAN, R. ; DUISTERMAAT, J.J.: Non-Hamiltonian Monodromy. In: *Journal of Differential Equations* 172 (2001), Nr. 1, 42 - 58. <http://dx.doi.org/http://dx.doi.org/10.1006/jdeq.2000.3852>. – DOI <http://dx.doi.org/10.1006/jdeq.2000.3852>. – ISSN 0022–0396
- [55] *Global Aspects of Classical Integrable Systems*. Birkhauser, 1997
- [56] A.G.USHVERIDZE: New Fundamental Symmetries of Integrable Systems and Partial Bethe Ansatz. In: *Annals of Physics* (1998)
- [57] GONZÁLEZ-LÁÑEZ, Artemio ; KAMRAN, Niky ; OLVER, Peter J.: New quasi-exactly solvable Hamiltonians in two dimensions. In: *Comm. Math. Phys.* 159 (1994), Nr. 3, 503–537. <http://projecteuclid.org/euclid.cmp/1104254730>
- [58] GONZALEZ-LOPEZ, Kamran N. A. ; OLVER, P.J.: Quasi-exact solvability. In: *Contemp. Math.* (1993)
- [59] GEOJO, K. G. ; SREE RANJANI, S. ; KAPOOR, A. K.: A study of quasi-exactly solvable models within the quantum Hamilton-Jacobi formalism. In: *Journal of Physics A Mathematical General* 36 (2003), April, S. 4591–4598. <http://dx.doi.org/10.1088/0305-4470/36/16/309>. – DOI 10.1088/0305–4470/36/16/309
- [60] EFSTATHIOU, K ; SUGNY, D: Integrable Hamiltonian systems with swallow-tails. In: *Journal of Physics A: Mathematical and Theoretical* 43 (2010), Nr. 8, 085216. <http://stacks.iop.org/1751-8121/43/i=8/a=085216>
- [61] SADOVSKIĀN, D.A. ; ZHILINSKIĀN, B.I.: Hamiltonian systems with detuned 1:1:2 resonance: Manifestation of bidromy. In: *Annals of Physics* 322 (2007), Nr. 1, 164 - 200. <http://dx.doi.org/http://dx.doi.org/10.1016/j.aop.2006.09.011>. – DOI <http://dx.doi.org/10.1016/j.aop.2006.09.011>. – ISSN 0003–4916. – January Special Issue 2007

# Appendix

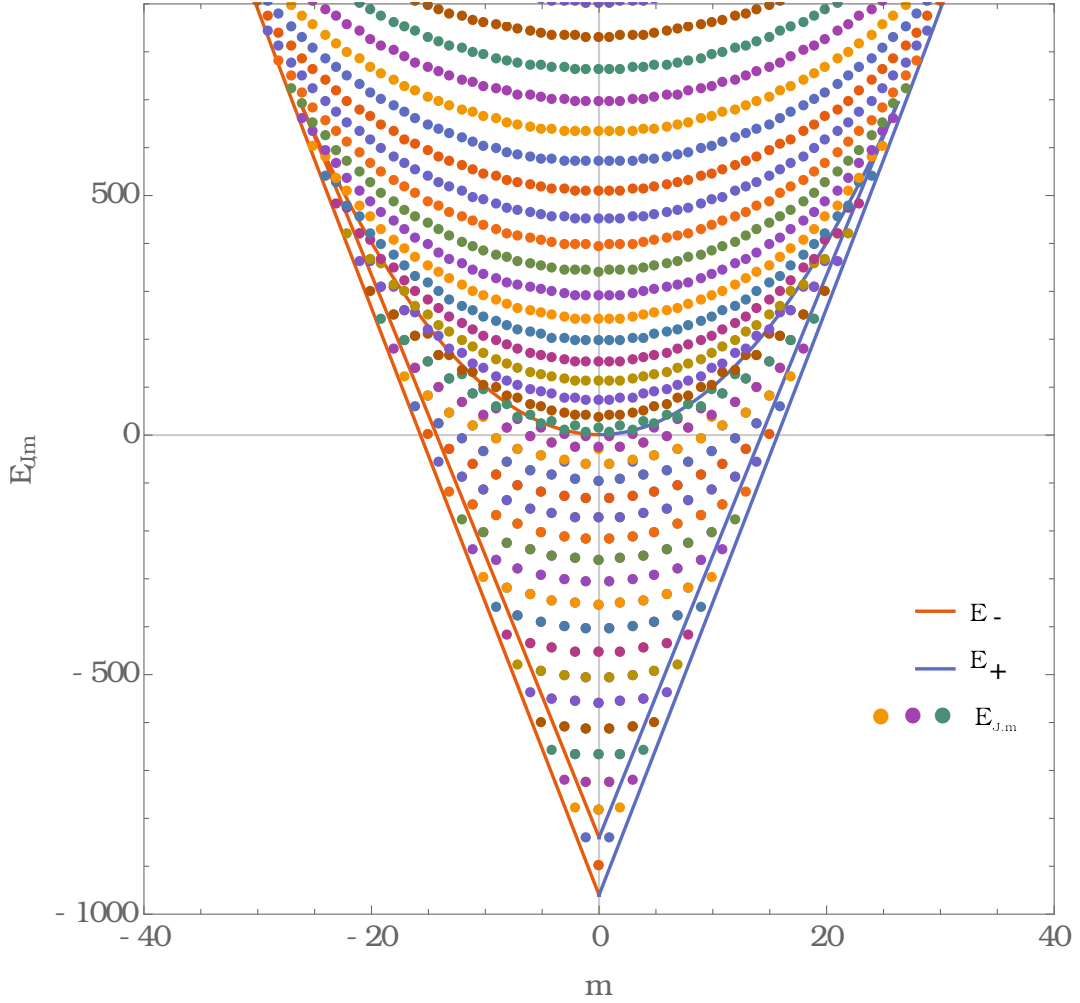


Figure 4.1: Energy-momentum map  $EM$  of the case 2 partner potential  $V_1^2$  and critical lines) for  $\beta = 30$  and  $k = 1$ . It can be seen that this system is equivalent to the quadratic pendulum

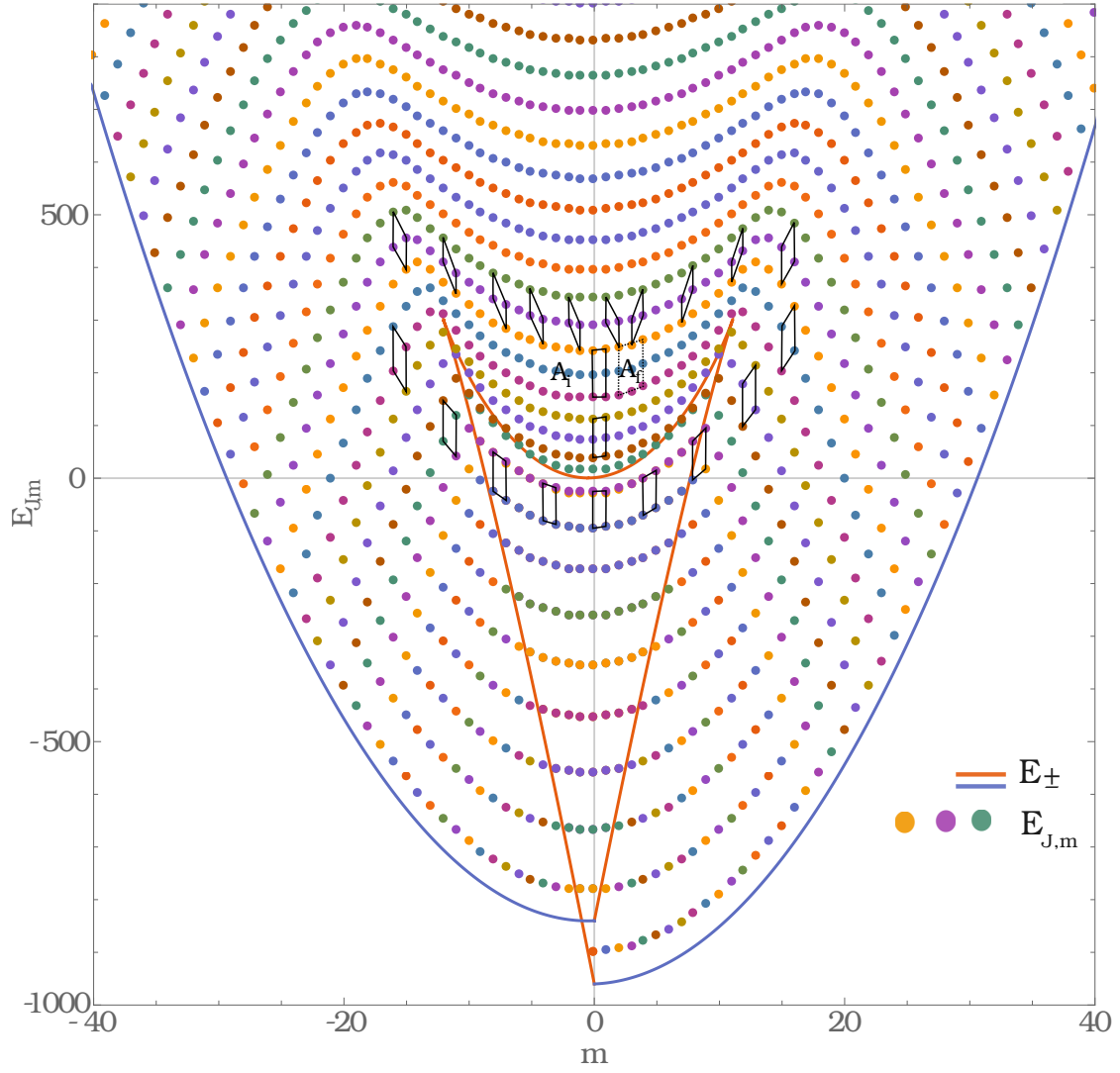


Figure 4.2: Energy-momentum map  $EM$  of the case  $1_-$  partner potential  $V_1^{1-}$  and critical lines for  $\beta = 30$  and  $k = m + 1$ . It can be seen that this system is equivalent to the quadratic pendulum

# Thanks

I want to thank Prof. Dr. Bretislav Friedrich for a very warm welcome at the Fritz-Haber-Institut der Max-Planck-Gesellschaft, being there to answer questions on a daily basis, providing many indispensable insights into the subject matter and beyond and for all the nice coffee that he knows to locate around town.

My thanks also go to Konrad Schatz, who helped me a lot with his thorough knowledge of the field and the many inspiring discussions on the topics of this thesis and helped motivate me, partially by not crushing me in our games of table tennis regularly, as he would surely have been able to do.

Prof Dr. Burkhardt Schmidt of the Freie-Universität Berlin was also very welcoming and helpful and I want to thank him for insights into aspects of the programming required, as well as very helpful discussions on the consequences of monodromy.

Last but not least, I would like to thank Prof. Dr. Alejandro Saenz of the Humboldt-Universität zu Berlin for supervising and grading this thesis.

# Selbständigkeitserklärung

Hiermit versichere ich, dass ich die vorliegende Arbeit selbständig verfasst und keine anderen als die angegebenen Quellen und Hilfsmittel verwendet habe.

Berlin, den 18. April 2016